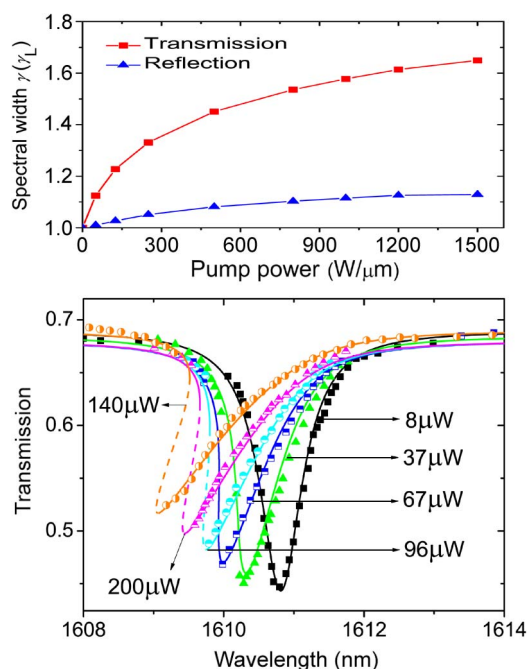


# Similar Role of Transient Kerr Effect and Two-Photon Absorption in a Nonlinear Photonic Crystal Nanocavity

Volume 5, Number 3, June 2013

Jun-Fang Wu  
Chao Li



DOI: 10.1109/JPHOT.2013.2262673  
1943-0655/\$31.00 ©2013 IEEE

# Similar Role of Transient Kerr Effect and Two-Photon Absorption in a Nonlinear Photonic Crystal Nanocavity

Jun-Fang Wu<sup>1,2</sup> and Chao Li<sup>1</sup>

<sup>1</sup>Engineering Research Center for Optoelectronics of Guangdong Province, Department of Physics, School of Science, South China University of Technology, Guangzhou 510640, China  
<sup>2</sup>State Key Laboratory of Luminescent Materials and Devices, South China University of Technology, Guangzhou 510640, China

DOI: 10.1109/JPHOT.2013.2262673  
1943-0655/\$31.00 ©2013 IEEE

Manuscript received April 10, 2013; revised May 1, 2013; accepted May 2, 2013. Date of publication May 13, 2013; date of current version May 21, 2013. This work was supported in part by the National Natural Science Foundation of China under Grant 11147111, by the Fundamental Research Funds for the Central Universities under Grant 2011ZM0086, and by the Strategic Emerging Industry Special Funds of Guangdong Province under Grants 2012A080302003 and 2012A080304015. Corresponding author: C. Li (e-mail: lichao@scut.edu.cn).

**Abstract:** The impacts of transient Kerr effect (TKE) on the characteristics of a nonlinear photonic crystal (PC) nanocavity are theoretically and numerically investigated. It is found that the features of TKE are very similar to those of two-photon absorption (TPA), but the mechanisms for them are essentially different. The relative magnitude of TKE to TPA is calculated, and the result indicates that the contribution of TKE should also be considered in actual designs of PC devices with Kerr nonlinearity. The theory presented in this paper will be helpful for the precise designs of nonlinear PC devices.

**Index Terms:** Nonlinear effects in nanostructures, ultrafast nonlinear processes, photonic crystals, nanocavities.

## 1. Introduction

With the development of integrated photonic systems, high-Q and small-volume nanocavities in two-dimensional (2-D) photonic crystals (PCs) have attracted much attention in recent years [1]–[3]. These resonant nanocavities are small enough to integrate and can be applied in extremely low-power nonlinear photonic devices because of their strong light-matter interactions. In such a nanocavity, several nonlinear effects such as Kerr effect, two-photon absorption (TPA), and free-carrier absorption (FCA) could be significantly strengthened [4]–[6], especially for those PC devices based on semiconductor materials, e.g., Si, Ge, and GaAs [6], [7]. So far, the dynamic features of Kerr effect, TPA, and FCA processes under the pump of ultrashort pulses have been well investigated and have been used for fabricating ultrafast all-optical switches [8], [9] or generating new frequencies [10], [11]. However, another dynamic process, say, the dynamic interaction between the continuous waves (CWs) and the nonlinear PC cavity, was seldom investigated [8]–[12]. Actually, under the pump of the CW light, the steady light field coupled in the cavity is oscillating at a frequency that is the same as the pump one. Considering that the response of nonresonant Kerr effect to optical pump is instantaneous [13]–[15], the Kerr-effect-induced change of the refractive index should also be very fast and periodical [16], [17], so we call this effect *transient Kerr effect* (TKE). As a result, the resonant frequency will oscillate harmonically between its initial position and a final position that is dependent on the pump intensity. This view has been testified by some

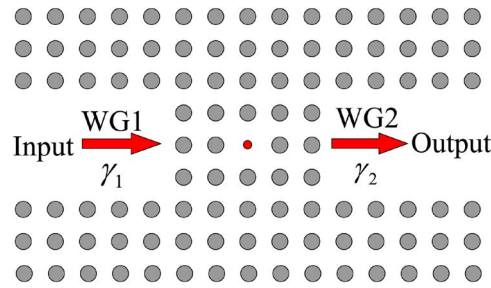


Fig. 1. Typical 2-D PC coupling system. WG1 and WG2 are input and output WGs, respectively, and the central point defect is resonant nanocavity with Kerr nonlinearity.

reported experiments [16], [17], but the related theoretical study is still deficient. Obviously, the transient shift of the resonant frequency will fundamentally affect the transmission and reflection features of a nonlinear PC cavity. Therefore, the investigation of the transient process under the pump of a CW light becomes very important and necessary.

In this paper, we will present an analytical model and numerical experiments to investigate the dynamic interaction between the CW light and the nonlinear PC cavity. Our results will show that the characteristics of TKE are very similar to those of TPA, and the underlying physical mechanism for this will be revealed.

## 2. Analytical Model for the Dynamic Interaction Inside a Nonlinear PC Cavity

Without loss of generality, we investigate for simplicity a typical 2-D PC coupling system whose cavity is nonlinear and is directly coupled to two waveguides (WGs), as shown in Fig. 1. The 2-D PC consists of a square lattice ( $15 \times 9$ ) of dielectric rods with a linear refractive index of  $n_0 = 3.4$ . Their radii are chosen to be  $0.2a$ , where  $a = 480$  nm is the lattice constant. The nonlinear PC cavity is created by reducing the radius of the central rod to  $0.1a$  and introducing Kerr nonlinearity ( $n_2 = 1 \times 10^{-5} \mu\text{m}^2/\text{W}$ ) into it. Two PC WGs are formed by cutting off three lines of rods and are symmetrically connected to the two ends of the nanocavity, respectively.

To clarify TKE and its impact more clearly, we suppose this PC structure has not any nonlinear absorption loss (e.g., TPA and FCA). As it is well known that in a linear case (the intensity of the CW pump light is ultralow), peak transmission is achieved only when the pump frequency is equal to the resonance one; once the pump frequency is off resonance, the transmission will drop sharply, and the transmission spectrum (i.e., the excited cavity mode) exhibits a Lorentzian line shape [14] in this linear case. If we suppose that the decay rates of the cavity mode amplitude into the input WG (WG1) and output WG (WG2) are  $\gamma_1$  and  $\gamma_2$ , respectively, and the intrinsic decay rate of the cavity is  $\gamma_0$  (which commonly originates from the linear absorption or radiation in a PC cavity), then the half of the linewidth of the cavity mode in this linear case is  $\gamma_L = \gamma_1 + \gamma_2 + \gamma_0$ .

However, with the increase in the pump intensity, under the influence of TKE, the resonant frequency will oscillate swiftly between its initial position and a final position that is dependent on the pump intensity. This means that the previous “off-resonance” components of the transmission spectrum will now have opportunities to experience the transient states of “on resonance” and therefore be strengthened. Thus, the linewidth of the excited cavity mode is broadened. Obviously, a bigger shift of the resonant frequency will offer more opportunities to those off-resonance components to experience “on-resonance” states, resulting in further broadening of the cavity mode in the frequency domain. We define this TKE-induced broadening quantity as  $\gamma_{\text{TKE}}$ , which is approximately proportional to the maximum shift of resonant frequency  $\Delta\omega_0$ . Thus, we have

$$\gamma_{\text{TKE}} = s_0 \Delta\omega_0 \quad (1)$$

where  $s_0$  is a dimensionless coefficient, and we call it *TKE-induced broadening parameter*. As will be shown below,  $s_0$  is a quasi-constant (equal to  $0.064 \pm 0.001$ ) and is almost independent of the power or frequency of the pump light. Moreover,  $s_0$  facilitates system design since a single

simulation is enough to determine it. As known from [15],  $\Delta\omega_0 = \gamma_L p_{\text{out}}/p_0$ , where  $p_{\text{out}}$  is the transmitted power, and  $p_0$  is the characteristic power that reflects the Kerr nonlinearity and the spatial confinement of the field in the cavity [15]. Accordingly,  $\gamma_{\text{TKE}}$  can be rewritten as  $\gamma_{\text{TKE}} = s_0 \gamma_L p_{\text{out}}/p_0$ , and the half of the linewidth of the resonant mode should be corrected as

$$\gamma = \gamma_L + \gamma_{\text{TKE}} = \gamma_L(1 + s_0 p_{\text{out}}/p_0). \quad (2)$$

When the nonlinear PC cavity is pumped by a CW light with frequency  $\omega$ , according to coupled mode theory (CMT) [18], the dynamic equation for the amplitude of the cavity mode can be written as

$$\begin{cases} dA/dt = [j(\omega_0 - \gamma p_{\text{out}}/p_0) - \gamma]A + \sqrt{2\gamma_1} s_{\text{in}} \\ p_{\text{out}} = 2\gamma_2 |A|^2 \\ s_{\text{in}} + s_R = \sqrt{2\gamma_1} A \end{cases} \quad (3)$$

where  $A$  is the mode amplitude to represent the electromagnetic energy  $|A|^2$  stored inside the cavity, and  $\omega_0$  is the resonant frequency of the cavity.  $s_{\text{in}}$  and  $s_R$  are the field amplitudes of the incident and reflective waves, respectively. Suppose the stable field of the incident CW light with frequency  $\omega$  has the form of  $s_{\text{in}} = |s_{\text{in}}(r)|e^{j\omega t}$ , where  $s_{\text{in}}(r)$  is the complex amplitude. Substituting the expression of  $s_{\text{in}}$  and (2) into (3) and noticing that  $A(0) = 0$  (in the initial moment, there is no energy inside the resonant cavity), the time-dependent nonlinear transmission coefficient  $T$  (defined as  $p_{\text{out}}/p_{\text{in}}$ , where  $p_{\text{in}} = |s_{\text{in}}|^2$  is the incident pump power) can be derived by using perturbation theory (here, the red shift of  $\omega_0$ , i.e., “ $-\gamma p_{\text{out}}/p_0$ ,” can be treated as a perturbation term since it is small enough in contrast with  $\omega_0$ )

$$A(t) = \frac{\sqrt{2\gamma_1} |s_{\text{in}}(r)|}{j(\omega_0 - \omega - \gamma p_{\text{out}}/p_0) - \gamma} \left[ e^{-\gamma t} \cdot e^{j(\omega_0 - \gamma p_{\text{out}}/p_0)t} - e^{j\omega t} \right] \quad (4)$$

$$T(t) = \frac{1}{(1 + s_0 p_{\text{out}}/p_0)^2} \cdot \frac{\eta}{(\delta - p_{\text{out}}/p_0)^2 + 1} \left\{ e^{-2\gamma t} - 2e^{-\gamma t} \cdot \cos[(\omega - \omega_0 + \gamma p_{\text{out}}/p_0)t] + 1 \right\} \quad (5)$$

where  $\delta = (\omega_0 - \omega)/\gamma_L$  is the frequency detuning of the incident CW with respect to the cavity mode, and  $\eta = 4\gamma_1 \gamma_2 / \gamma_L^2$  is the linear peak transmission coefficient when the pump intensity is ultralow.

From (4) and (5), one can see clearly that except for the frequency  $\omega$  of the incident light, the cavity mode with frequency “ $\omega_0 - \gamma p_{\text{out}}/p_0$ ” is also excited (where “ $-\gamma p_{\text{out}}/p_0$ ” is the red shift of the resonant frequency under the external pump), no matter in the cavity or in the transmitted light. However, this cavity mode will decay with time in rate of  $\gamma$ , as suggested by the term of “ $e^{-\gamma t}$ .” Equation (5) further shows that in the time domain,  $T$  will oscillate with period of  $2\pi/(\omega - \omega_0 + \gamma p_{\text{out}}/p_0)$  due to the interaction of the photons with different frequencies, i.e., pump frequency  $\omega$  and red-shifted resonant frequency “ $\omega_0 - \gamma p_{\text{out}}/p_0$ .” Obviously, the higher the pump power is, the greater the red shift “ $\gamma p_{\text{out}}/p_0$ ” will be, which implies a shorter oscillation period of  $T$ , as can be seen clearly in Fig. 2, where the dynamic evolution processes for the transmitted light in the time domain (under the excitations of different pump powers) are plotted.

When time is long enough, i.e., let  $t \rightarrow \infty$ , we obtain the stable transmission coefficient  $T$  from (5)

$$T = \frac{1}{(1 + s_0 p_{\text{out}}/p_0)^2} \cdot \frac{\eta}{(\delta - p_{\text{out}}/p_0)^2 + 1}. \quad (6)$$

Similarly, the stable reflection coefficient  $R$  (defined as  $|s_R|^2/p_{\text{in}}$ , where  $|s_R|^2$  denotes the reflected power) can also be derived

$$R = \frac{[(\gamma_1 - \gamma_2 - \gamma_0)/\gamma_L - s_0 p_{\text{out}}/p_0]^2 / (1 + s_0 p_{\text{out}}/p_0)^2 + (\delta - p_{\text{out}}/p_0)^2}{(\delta - p_{\text{out}}/p_0)^2 + 1}. \quad (7)$$

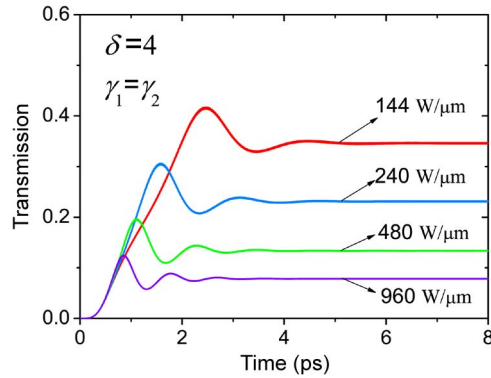


Fig. 2. Dynamic evolution of transmission for different pump powers, corresponding to  $\delta = 4$ ,  $\rho_0 = 8.64 \text{ W}/\mu\text{m}$ ,  $\gamma_0 = 0$ , and  $\gamma_1 = \gamma_2 = 1.16 \times 10^{-4} (2\pi c/a)$ .

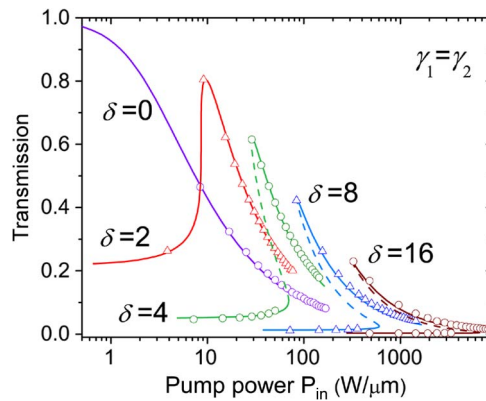


Fig. 3. Transmission versus pump power under the influence of TKE for different frequency detunings, corresponding to  $\gamma_1 = \gamma_2$ ,  $\gamma_0 = 0$ , and  $\rho_0 = 8.64 \text{ W}/\mu\text{m}$ .

If we let  $s_0 = 0$ , say, disregarding the TKE-induced broadening of the cavity mode, then the above nonlinear transmission and reflection formulas will immediately go back to the conventional forms, e.g., (6) becomes

$$T = \frac{\eta}{(\delta - \rho_{\text{out}}/\rho_0)^2 + 1} \quad (8)$$

which is exactly right the well-known transmission formula as proposed in [15].

In this way, the analytical model of TKE is established, and one shall see that nonzero  $s_0$  will play an important role in the nonlinear response of the PC cavity. Successively, based on this model, we will further investigate how TKE affects the characteristics of a nonlinear PC cavity, and some novel phenomena will be revealed.

### 3. Influences of TKE: The Similar Features of TKE and TPA

In this section, we will further reveal the impact of TKE on the characteristics of a nonlinear PC cavity. From (6), it is readily found that for a given frequency detuning  $\delta$ , when  $\rho_{\text{out}}/\rho_0 = \delta$ ,  $T$  will reach its peak value

$$T_{\text{max}} = \eta / (1 + s_0 \delta)^2. \quad (9)$$

Obviously,  $T_{\text{max}}$  is always less than  $\eta$  and decreases monotonously with the increase in frequency detuning  $\delta$ , as shown in Fig. 3 as solid curves, where the middle branch (dashed line) for

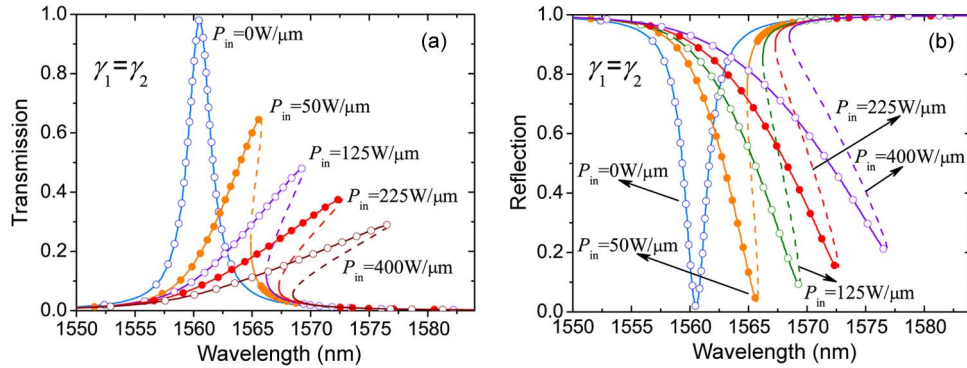


Fig. 4. Influence of TKE on (a) the transmission spectra and (b) reflection spectra for different pump powers. The theoretically calculated results are depicted as solid curves, and the FDTD simulation results are also plotted as open circles or dots for comparison purpose.

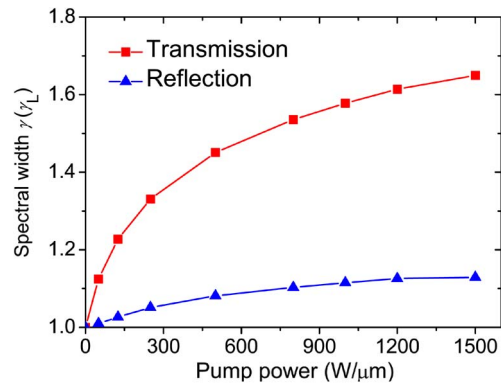


Fig. 5. Spectral widths of the transmitted and reflected light as functions of pump power.

each hysteresis curve is unstable so that even a tiny perturbation will cause the solution to decay to either the upper or lower branch. Simultaneously, it is also found that the critical pump power for beginning a bistable switching action increases when a bigger  $\delta$  is taken.

Successively, we further investigate the influence of TKE on the transmission and reflection spectra of the nonlinear PC cavity. According to (6) and (7), the transmission and reflection spectra for different pump powers are depicted in Fig. 4(a) and (b) as solid curves, respectively (the dashed line for each hysteresis curve denotes an unstable region). One can see clearly that under the influence of TKE, the center of the transmission/reflection spectrum is red shifted to a longer wavelength, and the cavity mode is broadened to an asymmetrical shape. In addition, it is also found that with the increase in the pump power, the red shifts of the transmission/reflection spectra become more and more significant, while the spectral widths become more and more broad, which results in the drop of the “height” for each transmission peak in Fig. 4(a) or the “depth” for each reflection valley in Fig. 4(b).

More importantly, by careful comparison between the transmission and reflection spectra, it is found that under the same pump condition, the spectral width of the transmitted light is always greater than that of the reflected one (they are equal only when the pump intensity is ultralow), and this difference increases when the pump power is further increased, as shown in Fig. 5.

These features of TKE predicted by analytical model can also be testified by numerical experiments. Here, we will utilize commercial software developed by RSoft Design Group ([www.rsoftdesign.com](http://www.rsoftdesign.com)) to perform nonlinear finite-difference time-domain (FDTD) simulations. As an example, we investigate for simplicity a lossless 2-D symmetric (i.e.,  $\gamma_1 = \gamma_2$  and  $\gamma_0 = 0$ ) PC

coupling system, as sketched in Fig. 1. The grid sizes in the horizontal and vertical directions are all chosen to be  $a/20$  (further reduction in grid size barely influences the simulation results), and a perfectly matched layer (PML) of  $1 \mu\text{m}$  is employed as the absorbing boundary. When the pump power is ultralow (say, in a linear case), a resonant mode with linewidth of  $\gamma_L = 2.32 \times 10^{-4}(2\pi c/a)$  is found to be located at  $\omega_0 = 0.3076(2\pi c/a)$  (or  $\lambda_0 = 1560 \text{ nm}$ ) in the first band gap for TM polarization, where  $c$  is the velocity of light in vacuum.

To obtain the upper hysteresis branch for transmission or the lower branch for reflection, each CW signal is superposed with an appropriate control light (the critical conditions of the control light can be found in [19]). The FDTD-simulated results are depicted as open circles or dots in Figs. 3 and 4; one can see that very good agreements are achieved between the theoretical predictions (solid curves) and FDTD simulation results (one should keep in mind that the dashed line for each hysteresis curve denotes an unstable region, where the states are actually unobservable in FDTD simulations or experiments, since even a tiny perturbation will cause them to decay to either the upper or lower states).

By substituting the data within the bistable region into (6) or (7),  $s_0$  and  $p_0$  can be calculated. Moreover, the calculations can be greatly simplified if we take advantage of some special points. For example, as suggested by (6), when  $p_{\text{out}}/p_0 = \delta$ ,  $T$  will reach its peak value  $T_{\text{max}} = \eta / (1 + s_0\delta)^2$ . Thus, for a given frequency detuning  $\delta$ ,  $s_0$  and  $p_0$  can be calculated by “ $s_0 = (\sqrt{\eta/T_{\text{max}}} - 1)/\delta$ ” and “ $p_0 = p_{\text{out}}/\delta = p_{\text{in}}T_{\text{max}}/\delta$ ,” respectively, where  $T_{\text{max}}$  and the corresponding pump power  $p_{\text{in}}$  can be directly read from Fig. 3. In this way,  $s_0$  and  $p_0$  are calculated to be  $(0.064 \pm 0.002)$  and  $8.64 \text{ W}/\mu\text{m}$ , respectively. Accordingly, it is verified again across all of the FDTD calculations in this paper that  $s_0$  is really a quasi-constant and is almost independent of the power or frequency of the pump light.

Now we see that TKE can fundamentally affect the characteristics of a nonlinear PC cavity. Actually, the aforementioned features of TKE (e.g., the red shift and broadening of the transmission/reflection spectrum, the reduction of the “height” for each transmission peak, or the “depth” for each reflection valley) are very similar to those of TPA as proposed in [7], [9], and [20], etc. To show this more clearly, let us make a further comparison between TKE and TPA. Normally, for a system with TPA, it is well known that the sum of transmission and reflection coefficients must be less than unity because of the existence of nonlinear absorption. However, for a system without TPA and with TKE only, can TKE exert the similar influence?

Using (6) and (7), the sum of transmission and reflection coefficients under the influence of TKE can be derived

$$T + R = 1 - \frac{4\gamma_1(\gamma_0 + \gamma_{\text{TKE}})/(\gamma_1 + \gamma_2 + \gamma_0 + \gamma_{\text{TKE}})^2}{(\delta - p_{\text{out}}/p_0)^2 + 1}. \quad (10)$$

From (10), one can see clearly that “ $T + R$ ” is always less than unity even for a lossless PC system (i.e.,  $\gamma_0 = 0$ ) once the TKE-induced broadening of the cavity mode cannot be neglected (i.e.,  $\gamma_{\text{TKE}} \neq 0$ ). Therefore, it is reasonable to phenomenologically introduce a “loss coefficient” into the PC cavity. Since this “loss coefficient” is induced by TKE, we thus call it *TKE-induced loss coefficient*, which can be written as

$$\alpha_{\text{TKE}} = 1 - T - R = \frac{4\gamma_1(\gamma_0 + \gamma_{\text{TKE}})/(\gamma_1 + \gamma_2 + \gamma_0 + \gamma_{\text{TKE}})^2}{(\delta - p_{\text{out}}/p_0)^2 + 1}. \quad (11)$$

Actually, this novel phenomenon can also be directly predicted by Fig. 5: Under the influence of TKE, the spectral widths for transmission and reflection will all be broadened, especially when the pump power is further increased. Considering that the energy is conserved in these spectral-broadening processes, the spectral broadening will result in the drop of the “height” for each transmission peak or the “depth” for each reflection valley. In other words, with the increase in the pump power, the transmission spectra will “fall” while the reflection spectra will “rise,” just as shown in Fig. 4. But, the spectral broadening of the transmitted light is greater than that of the

reflected one, especially when the pump power is high (see Fig. 5). As a result, the “fall” of the transmission spectrum is always greater than the “rise” of the reflection spectrum, so that the sum of  $T$  and  $R$  is always less than unity when TKE is taken into account.

Essentially, this novel phenomenon can also be well explained by (4) and (5): Under the pump of the incident CW light with frequency  $\omega$ , the cavity mode with frequency “ $\omega_0 - \gamma p_{\text{out}}/p_0$ ” is also excited and will decay with time in rate of  $\gamma$ . However, as known to all, either  $T$  or  $R$  is defined as the stable ratio of the transmitted power or reflective power to the input power *when time is long enough*, which means that the power of the excited cavity mode has been excluded from the calculations of  $T$  and  $R$ . That is why the sum of  $T$  and  $R$  is always less than unity, no matter for a nonlinear or a linear case (for the latter, the cavity mode will be excited at the frequency “ $\omega_0$ ” instead of “ $\omega_0 - \gamma p_{\text{out}}/p_0$ ”). So, it is not strange why the linear peak transmission  $\eta$  is always slightly less than unity (see Fig. 4). Of course, if we integrate the transmitted, reflected, and input powers *over the whole time domain* (so that the contribution of the excited cavity mode is also included) to calculate the total input and output energy values, one will find that the sum of the transmitted and reflected energy values is still equal to the input one since energy is conserved in such a lossless system.

In addition, as known from (11),  $\alpha_{\text{TKE}}$  will reach its maximum when  $p_{\text{out}}/p_0 = \delta$ , exactly right corresponding to a peak transmission. This phenomenon can be well understood: When  $p_{\text{out}}/p_0 = \delta$ , a “resonance” will occur [known by (6)], and the pump energy coupled into the cavity will be the maximum, so the shift of the resonant frequency  $\Delta\omega_0$  is also the maximum, resulting in a maximum  $\gamma_{\text{TKE}}$  [according to (1)], which indicates the strongest TKE and the greatest TKE-induced loss rate.

All these imply the similar role of TKE and TPA in a nonlinear PC cavity. It is a natural result since these two effects are all proportional to the intensity of the energy stored in cavity. However, the mechanisms for TKE and TPA are essentially different: The former is related with the real part of the nonlinear refractive coefficient, while the latter is determined by the imaginary part.

Successively, let us further analyze the relative magnitude of TKE compared with that of TPA in a Si system since in such a system Kerr effect and TPA are two dominant nonlinear effects [21], [22]. As known by (6) in [20],  $\gamma_{\text{TPA}}$  has the form of

$$\gamma_{\text{TPA}} = \frac{\beta c^2}{n_0^2 V_{\text{TPA}}} |A|^2 \quad (12)$$

where  $\beta$  is the TPA coefficient,  $c$  is the velocity of light in vacuum,  $|A|^2$  denotes the electromagnetic energy stored inside the cavity,  $n_0$  is the linear refractive index of Si, and  $V_{\text{TPA}}$  is the cavity volume for TPA and is approximately equal to  $4.9(\lambda/n_0)^3$  [9], [20].

According to (12) and the definition of  $\gamma_{\text{TKE}}$  in this paper, it is not difficult to obtain the ratio of  $\gamma_{\text{TKE}}$  to  $\gamma_{\text{TPA}}$  (here, the expression of  $p_0$  defined in [15] is introduced into the calculation)

$$\gamma_{\text{TKE}}/\gamma_{\text{TPA}} = \kappa_0 s_0 n_2 n_0^2 \omega_0^4 V_{\text{TPA}} / 4\beta c^4 \quad (13)$$

where  $\kappa_0$  is the nonlinear feedback parameter to describe the degree of spatial confinement of the field in the nonlinear cavity [15], and  $n_2$  is the real part of the nonlinear refractive coefficient. Noticing that the imaginary part of nonlinear refractive coefficient  $n_{2\text{Im}} = c\beta/2\omega_0$  [23], (13) can be rewritten as

$$\gamma_{\text{TKE}}/\gamma_{\text{TPA}} = \kappa_0 s_0 n_0^2 \omega_0^3 V_{\text{TPA}} n_2 / 8c^3 n_{2\text{Im}}. \quad (14)$$

Equation (14) indicates that this ratio is scale independent because of the product “ $\omega_0^3 V_{\text{TPA}}$ ” and is proportional to the relative magnitude of the real part to the imaginary part of the nonlinear refractive coefficient. If we use the corresponding data presented in [20] and substitute them into (13), the ratio is approximately calculated to be nearly 0.20. Therefore, in actual designs of PC devices with Kerr nonlinearity, the influence of TKE should also be considered.

The contribution of TKE to nonlinear transmission and reflection can also be reflected by several proposed experimental results. For example, in [24], an all-optical bistable switching in PC



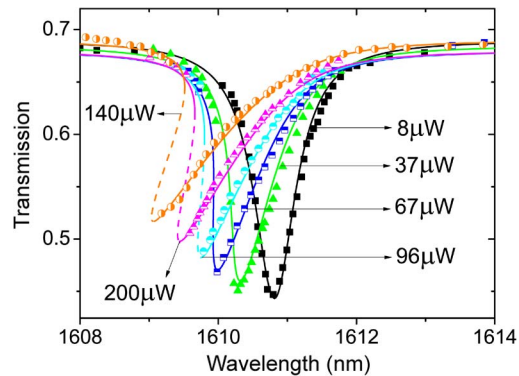


Fig. 6. Fitting of the experimental data based on the analytical model of TKE. The theoretical curves calculated by TKE theory are plotted as solid lines, and the experimental data extracted from Fig. 3(a) in [24] are plotted as discrete dots, for comparison purpose.

resonators with Kerr nonlinearity is investigated experimentally and theoretically. One can see that the measured transmission spectra for different pump powers, i.e., Fig. 3(a) in [24], are very similar to Fig. 4(b) calculated by the analytical model in our work<sup>1</sup> but are not in good accord with the transmission spectra calculated by their own model [see Fig. 3(b) in [24], where only conventional Kerr effect is considered]. This discrepancy is mainly embodied in two aspects. First, the “blue shift” of the transmission spectrum calculated by their model is much greater than the measured one. Second, the analytical model with conventional Kerr effect cannot explain why the “valley” of the transmission spectrum will rise with the increase in the pump power (their theoretically calculated “valley” keeps invariant). However, if we take the contribution of TKE into account, the aforementioned discrepancy can be well explained: i) The TKE-induced loss will further lower the optical energy stored in the cavity, which leads to the reduction of the blue shift of the cavity mode (since the blue shift is proportional to the energy stored in cavity); ii) the rise of the “valley” of the transmission spectrum is just one of the features of TKE, as has been discussed before.<sup>1</sup>

Now, let us directly testify the analytical model of TKE by using the experimental data. According to the data extracted from the measured transmission spectra in Fig. 3(a) in [24],  $s_0$  and  $p_0$  are calculated to be “ $-0.043$ ” and “ $-3.65 \mu\text{W}$ ,” respectively (note that  $n_2 < 0$  in this case);  $\gamma_1 = \gamma_2 = 1.08 \times 10^{-5}$ , and  $\gamma_0 = 4.33 \times 10^{-5}$ . In Fig. 6, the theoretical curves calculated by TKE theory are plotted as solid lines, and the experimental data extracted from Fig. 3(a) in [24] are plotted as discrete dots, for comparison purpose. One can see that the experimental results are precisely predicted by TKE theory. This further shows that the analytical model of TKE is effect and can be naturally extended to real 3-D cases with Kerr nonlinearity.

#### 4. Conclusion

In summary, we have established a physical model to investigate the impacts of TKE on the characteristics of a nonlinear PC nanocavity, and the theoretical predictions agree with the numerical experiment results quite well. It is found that the features of TKE are very similar to those of TPA, but the mechanisms for them are essentially different. The relative magnitude of TKE to TPA is calculated and is found to be proportional to the ratio of the real part to the imaginary part of the nonlinear refractive coefficient. In addition, based on the analytical model presented in this paper, the unexpected discrepancy between the experimental and the analytical results in some references can be well explained. The theory of TKE and the discussion on it will be helpful for the precise designs of nonlinear PC devices.

<sup>1</sup>In [24], the resonant cavity is side coupled to the WG, while in our case, they are directly coupled, so that the transmission spectra presented in [24] correspond to the reflection spectra presented in our work and *vice versa*. Besides, in [24], the nonlinear refractive index  $n_2$  is negative, while in our case, it is positive, so that with the increase in the pump power, the transmission spectra in [24] are blue shifted, while in our case, the spectra are red shifted.

## Acknowledgment

The authors wish to thank the anonymous reviewers for their valuable suggestions.

## References

- [1] Y. Akahane, T. Asano, B. S. Song, and S. Noda, "High-Q photonic nanocavity in a two-dimensional photonic crystal," *Nature*, vol. 425, no. 6961, pp. 944–947, Oct. 2003.
- [2] M. Notomi, A. Shinya, S. Mitsugi, G. Kira, E. Kuramochi, and T. Tanabe, "Optical bistable switching action of Si high-Q photonic-crystal nanocavities," *Opt. Exp.*, vol. 13, no. 7, pp. 2678–2687, Apr. 2005.
- [3] X. D. Yang, C. Husko, and C. W. Wong, "Digital resonance tuning of high-Q/ $V_m$  silicon photonic crystal nanocavities by atomic layer deposition," *Appl. Phys. Lett.*, vol. 91, no. 16, pp. 161114-1–161114-3, Oct. 2007.
- [4] K. Nozaki, T. Tanabe, A. Shinya, S. Matsuo, T. Sato, H. Taniyama, and M. Notomi, "Sub-femtojoule all-optical switching using a photonic-crystal nanocavity," *Nat. Photon.*, vol. 4, no. 7, pp. 477–483, Jul. 2010.
- [5] J. Bravo-Abad, A. Rodriguez, P. Bermel, S. G. Johnson, J. D. Joannopoulos, and M. Soljacic, "Enhanced nonlinear optics in photonic-crystal microcavities," *Opt. Exp.*, vol. 15, no. 24, pp. 16 161–16 176, Nov. 2007.
- [6] J. Bravo-Abad, E. P. Ippen, and M. Soljacic, "Ultrafast photodetection in an all-silicon chip enabled by two-photon absorption," *Appl. Phys. Lett.*, vol. 94, pp. 241103-1–241103-3, Jun. 2009.
- [7] E. Weidner, S. Combrie, A. de Rossi, N. V. Q. Tran, and S. Cassette, "Nonlinear and bistable behavior of an ultrahigh-Q GaAs photonic crystal nanocavity," *Appl. Phys. Lett.*, vol. 90, no. 10, pp. 101118-1–101118-3, Mar. 2007.
- [8] P. J. Harding, T. G. Euser, Y. R. Nowicki-Bringuier, J. M. Gerard, and W. L. Vos, "Dynamical ultrafast all-optical switching of planar GaAs/AlAs photonic microcavities," *Appl. Phys. Lett.*, vol. 91, no. 11, pp. 111103-1–111103-3, Sep. 2007.
- [9] P. E. Barclay, K. Srinivasan, and O. Painter, "Nonlinear response of silicon photonic crystal microresonators excited via an integrated waveguide and fiber taper," *Opt. Exp.*, vol. 13, no. 3, pp. 801–820, Feb. 2005.
- [10] S. F. Preble, Q. F. Xu, and M. Lipson, "Changing the colour of light in a silicon resonator," *Nat. Photon.*, vol. 1, no. 5, pp. 293–296, May 2007.
- [11] T. Tanabe, M. Notomi, H. Taniyama, and E. Kuramochi, "Dynamic release of trapped light from an ultrahigh-Q nanocavity via adiabatic frequency tuning," *Phys. Rev. Lett.*, vol. 102, no. 4, pp. 043907-1–043907-4, Jan. 2009.
- [12] T. G. Euser, A. J. Molenaar, J. G. Fleming, B. Gralak, A. Polman, and W. L. Vos, "All-optical octave-broad ultrafast switching of Si woodpile photonic band gap crystals," *Phys. Rev. B, Condens. Matter*, vol. 77, no. 11, pp. 115214-1–115214-6, Mar. 2008.
- [13] M. F. Yanik, S. H. Fan, and M. Soljacic, "High-contrast all-optical bistable switching in photonic crystal microcavities," *Appl. Phys. Lett.*, vol. 83, no. 14, pp. 2739–2741, Oct. 2003.
- [14] J. D. Joannopoulos, R. D. Meade, and J. N. Winn, *Photonic Crystals: Molding the Flow of Light*. Princeton, NJ, USA: Princeton Univ. Press, 1995.
- [15] M. Soljacic, M. Ibanescu, S. G. Johnson, Y. Fink, and J. D. Joannopoulos, "Optimal bistable switching in nonlinear photonic crystals," *Phys. Rev. E, Stat., Nonlin., Soft Matter Phys.*, vol. 66, no. 5, pp. 055601-1–055601-4, Nov. 2002.
- [16] E. Yüce, G. Ctistis, J. Claudon, E. Dupuy, R. D. Buijs, B. de Ronde, A. P. Mosk, J.-M. Gérard, and W. L. Vos, "All-optical switching of a microcavity repeated at terahertz rates," *Opt. Lett.*, vol. 38, no. 3, pp. 374–376, Feb. 2013.
- [17] G. Ctistis, E. Yüce, A. Hartsuiker, J. Claudon, M. Bazin, J.-M. Gérard, and W. L. Vos, "Ultimate fast optical switching of a planar microcavity in the telecom wavelength range," *Appl. Phys. Lett.*, vol. 98, no. 16, pp. 161114-1–161114-3, Apr. 2011.
- [18] H. A. Haus, *Waves and Fields in Optoelectronics*. Englewood Cliffs, NJ, USA: Prentice-Hall, 1984.
- [19] C. Li, H. Wang, J. F. Wu, and W. C. Xu, "Critical conditions of control light for a silicon-based photonic crystal bistable switching," *Opt. Exp.*, vol. 18, no. 16, pp. 17 313–17 321, Aug. 2010.
- [20] T. Uesugi, B. S. Song, T. Asano, and S. Noda, "Investigation of optical nonlinearities in an ultra-high-Q Si nanocavity in a two-dimensional photonic crystal slab," *Opt. Exp.*, vol. 14, no. 1, pp. 377–386, Jan. 2006.
- [21] G. Priem, P. Bienstman, G. Morthier, and R. Baets, "Impact of absorption mechanisms on Kerr-nonlinear resonator behavior," *J. Appl. Phys.*, vol. 99, no. 6, pp. 063103-1–063103-8, Mar. 2006.
- [22] D. Brissinger, B. Cluzel, A. Coillet, C. Dumas, P. Grelu, and F. de Formel, "Near-field control of optical bistability in a nanocavity," *Phys. Rev. B, Condens. Matter*, vol. 80, no. 3, pp. 033103-1–033103-4, Jul. 2009.
- [23] N. Suzuki, "FDTD analysis of two-photon absorption and free-carrier absorption in Si high-index-contrast waveguides," *J. Lightwave Technol.*, vol. 25, no. 9, pp. 2495–2501, Sep. 2007.
- [24] M.-K. Kim, I.-K. Hwang, S.-H. Kim, H.-J. Chang, and Y.-H. Lee, "All-optical bistable switching in curved microfiber-coupled photonic crystal resonators," *Appl. Phys. Lett.*, vol. 90, no. 16, pp. 161118-1–161118-3, Apr. 2007.